

Single mode step-index polymer optical fiber for humidity insensitive high temperature fiber Bragg grating sensors

Getinet Woyessa,^{1,*} Andrea Fasano,² Alessio Stefani,^{1,3} Christos Markos,^{1,4} Kristian Nielsen,¹ Henrik K. Rasmussen,² and Ole Bang¹

¹DTU Fotonik, Department of Photonics Engineering, Technical University of Denmark, DK-2800 Kgs. Lyngby, Denmark

²DTU Mekanik, Department of Mechanical Engineering, Technical University of Denmark, DK-2800 Kgs. Lyngby, Denmark

³Institute of Photonics and Optical Science (IPOS), School of Physics, The University of Sydney, NSW 2006, Australia.

⁴CREOL, The College of Optics & Photonics, University of Central Florida, 4000 Central Florida Blvd., Orlando, FL 32816, USA

*gewoy@fotonik.dtu.dk

Abstract: We have fabricated the first single-mode step-index and humidity insensitive polymer optical fiber operating in the 850 nm wavelength ranges. The step-index preform is fabricated using injection molding, which is an efficient method for cost effective, flexible and fast preparation of the fiber preform. The fabricated single-mode step-index (SI) polymer optical fiber (POF) has a 4.8 μ m core made from TOPAS grade 5013S-04 with a glass transition temperature of 134°C and a 150 μ m cladding made from ZEONEX grade 480R with a glass transition temperature of 138°C. The key advantages of the proposed SIPOF are low water absorption, high operating temperature and chemical inertness to acids and bases and many polar solvents as compared to the conventional poly-methyl-methacrylate (PMMA) and polystyrene based POFs. In addition, the fiber Bragg grating writing time is short compared to microstructured POFs.

©2016 Optical Society of America

OCIS codes: (060.2280) Fiber design and fabrication, (130.5460) Polymer waveguides, (060.2270) Fiber characterization, (060.3735) Fiber Bragg gratings, (060.2370) Fiber optics sensors.

References and links

1. T. Kaino, M. Fujiki, and S. Nara, "Low-loss polystyrene core-optical fibers," *J. Appl. Phys.* **52**(12), 7061–7063 (1981).
2. T. Kaino, M. Fujiki, S. Oikawa, and S. Nara, "Low-loss plastic optical fibers," *Appl. Opt.* **20**(17), 2886–2888 (1981).
3. Y. Koike and M. Asai, "The future of plastic optical fiber," *NPG Asia Mater.* **1**(1), 22–28 (2009).
4. K. Peters, "Polymer optical fiber sensors – a review," *Smart Mater. Struct.* **20**(1), 013002 (2011).
5. D. J. Webb, "Fiber Bragg grating sensors in polymer optical fibers," *Meas. Sci. Technol.* **26**(9), 092004 (2015).
6. D. J. Webb and K. Kalli, "Polymer fiber bragg gratings," in *Fiber Bragg Grating Sensors: Thirty Years From Research to Market*, A. Cusano, A. Cutolo, and J. Albert eds. (Bentham Science, 2010).
7. J. Jensen, P. Hoiby, G. Emiliyanov, O. Bang, L. Pedersen, and A. Bjarklev, "Selective detection of antibodies in microstructured polymer optical fibers," *Opt. Express* **13**(15), 5883–5889 (2005).
8. G. Emiliyanov, J. B. Jensen, O. Bang, P. E. Hoiby, L. H. Pedersen, E. M. Kjaer, and L. Lindvold, "Localized biosensing with Topas microstructured polymer optical fiber," *Opt. Lett.* **32**(5), 460–462 (2007).
9. C. Markos, W. Yuan, K. Vlachos, G. E. Town, and O. Bang, "Label-free biosensing with high sensitivity in dual-core microstructured polymer optical fibers," *Opt. Express* **19**(8), 7790–7798 (2011).
10. H. Dobb, D. J. Webb, K. Kalli, A. Argyros, M. C. J. Large, and M. A. van Eijkelenborg, "Continuous wave ultraviolet light-induced fiber Bragg gratings in few- and single-mode microstructured polymer optical fibers," *Opt. Lett.* **30**(24), 3296–3298 (2005).

11. Z. Xiong, G. D. Peng, B. Wu, and P. L. Chu, "Highly tunable Bragg gratings in single-mode polymer optical fibers," *IEEE Photonics Technol. Lett.* **11**(3), 352–354 (1999).
12. A. Stefani, S. Andresen, W. Yuan, N. Herholdt-Rasmussen, and O. Bang, "High sensitivity polymer optical fiber-Bragg-grating-based accelerometer," *IEEE Photonics Technol. Lett.* **24**(9), 763–765 (2012).
13. G. D. Peng, P. L. Chu, Z. Xiong, T. W. Whitbread, and R. P. Chaplin, "Dye-Doped Step-Index Polymer Optical Fiber for Broadband Optical Amplification," *J. Lightwave Technol.* **14**(10), 2215–2223 (1996).
14. G. Zhou, C.-F. J. Pun, H. Tam, A. C. L. Wong, C. Lu, and P. K. A. Wai, "Single-Mode Perfluorinated Polymer Optical Fibers With Refractive Index of 1.34 for Biomedical Applications," *IEEE Photonics Technol. Lett.* **22**(2), 106–108 (2010).
15. Y. Koike, Y. Takezawa, and Y. Ohtsuka, "New interfacial-gel copolymerization technique for steric GRIN polymer optical waveguides and lens arrays," *Appl. Opt.* **27**(3), 486–491 (1988).
16. M. Beckers, T. Schlüter, T. Vad, T. Gries, and C.-A. Bunge, "An overview on fabrication methods for polymer optical fibers," *Polym. Int.* **64**(1), 25–36 (2015).
17. M. van Eijkelenborg, M. Large, A. Argyros, J. Zagari, S. Manos, N. Issa, I. Bassett, S. Fleming, R. McPhedran, C. M. de Sterke, and N. A. Nicorovici, "Microstructured polymer optical fibre," *Opt. Express* **9**(7), 319–327 (2001).
18. A. Stefani, W. Yuan, C. Markos, and O. Bang, "Narrow bandwidth 850 nm fiber Bragg gratings in few-mode polymer optical fibers," *IEEE Photonics Technol. Lett.* **23**(10), 660–662 (2011).
19. A. Abang and D. J. Webb, "Demountable connection for polymer optical fiber grating sensors," *Opt. Eng.* **51**(8), 080503 (2012).
20. G. D. Marshall, D. J. Kan, A. A. Asatryan, L. C. Botten, and M. J. Withford, "Transverse coupling to the core of a photonic crystal fiber: the photo-inscription of gratings," *Opt. Express* **15**(12), 7876–7887 (2007).
21. I.-L. Bundalo, K. Nielsen, and O. Bang, "Angle dependent Fiber Bragg grating inscription in microstructured polymer optical fibers," *Opt. Express* **23**(3), 3699–3707 (2015).
22. H. G. Harbach, "Fiber Bragg gratings in polymer optical fibers," PhD Thesis, Lausanne, EPFL (2008).
23. C. Zhang, W. Zhang, D. J. Webb, and G. D. Peng, "Optical fiber temperature and humidity sensor," *Electron. Lett.* **46**(9), 643–644 (2010).
24. G. Khanarian and H. Celanese, "Optical properties of cyclic olefin copolymers," *Opt. Eng.* **40**(6), 1024–1029 (2001).
25. <http://www.zeonex.com>
26. <http://www.topas.com>
27. I. P. Johnson, W. Yuan, A. Stefani, K. Nielsen, H. K. Rasmussen, L. Khan, D. J. Webb, K. Kalli, and O. Bang, "Optical fiber Bragg grating recorded in TOPAS cyclic olefin copolymer," *Electron. Lett.* **47**(4), 271–272 (2011).
28. W. Yuan, L. Khan, D. J. Webb, K. Kalli, H. K. Rasmussen, A. Stefani, and O. Bang, "Humidity insensitive TOPAS polymer fiber Bragg grating sensor," *Opt. Express* **19**(20), 19731–19739 (2011).
29. C. Markos, A. Stefani, K. Nielsen, H. K. Rasmussen, W. Yuan, and O. Bang, "High-Tg TOPAS microstructured polymer optical fiber for fiber Bragg grating strain sensing at 110 degrees," *Opt. Express* **21**(4), 4758–4765 (2013).
30. K. Nielsen, H. K. Rasmussen, A. J. L. Adam, P. C. M. Planken, O. Bang, and P. U. Jepsen, "Bendable, low-loss Topas fibers for the terahertz frequency range," *Opt. Express* **17**(10), 8592–8601 (2009).
31. I. Anthony, R. Leonhardt, A. Argyros, and M. C. J. Large, "Characterization of a microstructured Zeonex terahertz fiber," *J. Opt. Soc. Am. B* **28**(5), 1013–1018 (2011).
32. Y. Zhang, K. Li, L. Wang, L. Ren, W. Zhao, R. Miao, M. C. J. Large, and M. A. van Eijkelenborg, "Casting preforms for microstructured polymer optical fibre fabrication," *Opt. Express* **14**(12), 5541–5547 (2006).
33. <https://www.thorlabs.com/thorcat/6800/780HP-SpecSheet.pdf>
34. <https://www.thorlabs.com/thorcat/22100/SM800G80-SpecSheet.pdf>
35. A. Stefani, K. Nielsen, H. K. Rasmussen, and O. Bang, "Cleaving of TOPAS and PMMA microstructured polymer optical fibers: Core-shift and statistical quality optimization," *Opt. Commun.* **285**(7), 1825–1833 (2012).
36. I.-L. Bundalo, K. Nielsen, C. Markos, and O. Bang, "Bragg grating writing in PMMA microstructured polymer optical fibers in less than 7 minutes," *Opt. Express* **22**(5), 5270–5276 (2014).
37. R. Oliveira, L. Bilro, and R. Nogueira, "Bragg gratings in a few mode microstructured polymer optical fiber in less than 30 seconds," *Opt. Express* **23**(8), 10181–10187 (2015).
38. I. P. Johnson, K. Kalli, and D. J. Webb, "827nm Bragg grating sensor in multimode microstructured polymer optical fiber," *Electron. Lett.* **46**(17), 1217–1218 (2010).

1. Introduction

A lot of research has gone into developing low loss polymer optical fibers (POFs) [1,2]. Mostly, it has been the area of short range communication that has been driving the research, development and commercialization of POFs, which now have a consolidated place in this field [3]. Loss in POFs has nevertheless been far from reaching that of silica fibers, in particular when it comes to single-mode fibers. However, POFs unique properties, such as

their very low processing temperature, high flexibility in bending, high fracture toughness, ease of handling, and non-brittle nature compared to glass fibers have now moved the interest about POFs towards the sensing field, where loss is not so crucial [4–6]. Biocompatibility further makes POFs ideal candidates for bio-sensing applications [7–9] and properties, such as a high elastic strain limit and low Young's modulus, makes it ideal for fiber Bragg grating based sensors [5,6], in particular in high strain and acceleration sensing applications [10–12]. Various types of POFs have been demonstrated so far, such as step-index [1,13,14], graded-index [2,15,16] and microstructured [17] POFs. In the quest for low loss POFs, highly multimode step-index and graded-index fibers have been developed and are now available commercially and widely used in short-range communication. However, single-mode fibers are necessary for FBG sensors. In order to obtain single-mode guidance, several fabrication techniques have been proposed: from reducing the diameter of commercially available graded-index fibers by re-drawing [14] to exploiting the endlessly single-mode behavior of microstructured optical fibers [17]. Single-mode step-index POFs have been available commercially, but they were very lossy (500 dB/m @ 850nm) and multi-mode at 850 nm because they were targeted to operate at 1550 nm (MORPOF02, Paradigm Optics, see [18]). However, POFs have lowest loss at visible wavelengths and only microstructured POFs have so far been demonstrated to be single-mode in this regime. The re-drawn commercial fiber presented in [14] was targeted to have single mode guidance at 1300nm and 1550nm.

Despite microstructured POFs being a good way of getting single-mode operation in the visible, solid fibers are preferable because this eliminates problems with (1) loss and degradation due to impurities getting into the holes, (2) the difficult to avoid loss due to scattering at the hole walls, and (3) cleaving, splicing, and connectorizing a fiber with holes in it [19]. Furthermore, in FBG sensor fabrication the holes of a microstructured POF strongly increased the writing time and quality of the grating due to scattering at the many- air-material interfaces [20,21].

Step-index and graded-index POFs that have been fabricated in the past are mostly PMMA or PS based [1,2,13,15,16] and therefore have low operating temperature and strong affinity for water, which makes them sensitive to humidity [22,23]. Thus, the strain and temperature response of FBG sensors based on these fibers will have a strong dependence on humidity.

As for the realization of the all-solid preform and/or fiber, techniques, such as batch extrusion, continuous extrusion, interfacial-gel polymerization, chemical vapor deposition, and centrifugation have been used [13–16]. Using these methods, fabrication of single mode POFs is difficult because it is not easy to control dopant diffusion from core to cladding during the polymerization of monomers in the preform making process. Thus, it is not easy to maintain the refractive index profile of POFs to ensure single-mode operation. In addition, these techniques are complex and time consuming. As a result, at the moment it is not possible to commercially buy a single-mode POF.

Here we demonstrate the first solid step-index POF, which is single-mode at 850 nm and which is humidity insensitive. The fiber is made of a TOPAS core and a ZEONEX cladding. Both materials are humidity insensitive and can operate at high temperature, because of their glass transition temperature exceeding 130°C. An injection molding technique has been used to fabricate the step index preform and heat drawing has been used for fiber fabrication. The fabricated fiber has a core size and a numerical aperture very close to that of a silica single mode fiber at the same wavelength, which is optimal for coupling. Moreover, since the main application for the fabricated fiber is FBG sensors, we also report the successful inscription and characterization of FBGs in the SIPOF.

2. TOPAS/ZEONEX step index POF fabrication

The SIPOF was fabricated in-house at DTU Fotonik. The preparation of the preform consisted of two steps: casting of the cladding material, ZEONEX, and injection molding of the core material, TOPAS. These two materials were chosen for the following reasons:

- They have very close chemical, mechanical and optical properties: as TOPAS is a cyclic olefin copolymer (COC) and ZEONEX is a cyclic-olefin polymer (COP).
- The selected grades of these polymers have almost the same glass transition temperature and very close refractive indices, with the refractive index of TOPAS 5013S-04 being slightly higher than that of ZEONEX 480R.
- These polymers are also a class of optical thermoplastics that are chemically inert to acids and bases and many polar solvents, have a very low moisture uptake, low birefringence, and superior moldability [24–26].
- FBG writing has been successfully demonstrated in different grades of TOPAS fibers and proved to be humidity insensitive, which makes them a potential candidate for humidity insensitive FBG sensors [27–29].
- TOPAS and ZEONEX have also good transparency at THz frequencies [30,31].

We started the preform fabrication by casting the cladding material, ZEONEX 480R produced by ZEON CORPORATION with a glass transition temperature of 138°C [25], from granulates into a solid rod. This method differs from chemical casting [32] as it does not involve any polymerization process. This polymer is suitable for engineering applications requiring mechanical stability at high temperature. After casting, the solid rod was machined to a uniform bulk preform of 60 mm diameter and 100 mm length. Then a single hole with a diameter of 4 mm was drilled at the center of the preform. In the second stage of the SI preform preparation TOPAS 5013S-04 was injected into the 4 mm hole. TOPAS 5013S-04 granulate was purchased from TOPAS Advanced Polymers and it has a glass transition temperature of 134°C [26]. An Engel ES 80/25 HL-Victory injection molding machine was used for injecting TOPAS into the host ZEONEX preform. Different injection temperatures were preliminarily tested. The aim was to optimize the transparency of the molten polymer before injection. This was done by visually inspecting the clarity of TOPAS while exiting the injection nozzle. Despite that a decrease in the injection temperature was seen to improve the transparency of the molten TOPAS, it was not possible to lower the temperature too much since TOPAS became too stiff to be processed. The optimal injection temperature was found to be around 200°C. Thereafter TOPAS was injection molded into the central hole of the ZEONEX solid rod with a melt pressure at the nozzle being slightly lower than the machine limit, which is approximately 2000 bar. The SI preform was then first drawn to a 5 mm cane. Then the 5 mm cane was sleeved and drawn to a fiber of 150 ± 3 μm diameter. The corresponding core diameter of the fiber is 4.8 μm . The end facet of the fabricated SIPOF is shown as inset in Fig. 1 (a).

3. TOPAS/ZEONEX single mode step index POF characterization

3.1 Refractive index profile and loss measurement

The refractive index contrast was measured at Azpect Photonics by interferometric optical phase measurement techniques with an accuracy of ± 0.0001 . Figure 1(a) shows the measured refractive index contrast of this SIPOF. The core has a refractive index, which is 0.00591 larger than that of the cladding. With this refractive index difference and a core size of 4.8 μm , the numerical aperture of the fiber is 0.13 and the normalized frequency is 2.38 at 850 nm. The measured core/cladding eccentricity is less than 0.6 μm and the nominal mode field diameter of this fiber is 5.3 ± 0.3 μm . The geometrical and optical parameters of the fiber are

closely matching those of silica single mode fibers operating in 850 nm region [33,34], allowing for easy coupling and low coupling loss between these fibers.

The transmission loss of the fabricated SIPOF was measured using the cut-back method. One end of the SIPOF was connectorized with a single mode silica patch cable, which was connected to a supercontinuum source (SuperK Extreme, NKT Photonics). The other end of the fiber was butt-coupled to an optical spectrum analyzer (OSA, Ando AQ6315A) via a standard silica single mode fiber to record the SIPOF transmission spectrum. The end facet of the fiber was cleaved with a custom-made cleaver at a temperature of 76°C for both the blade and the fiber [35]. The fiber was cut-back from 5 m to 30 cm; recording the transmission spectrum of over 40 different fiber cuts in order to eliminate any uncertainties arising from power fluctuations, cleave quality and so on. The measured loss profile of the TOPAS SIPOF is shown in Fig. 1 (b). The minimum loss was found to be 4.197 dB/m at 862 nm. The fiber attenuation at 850 nm is 4.55 dB/m.

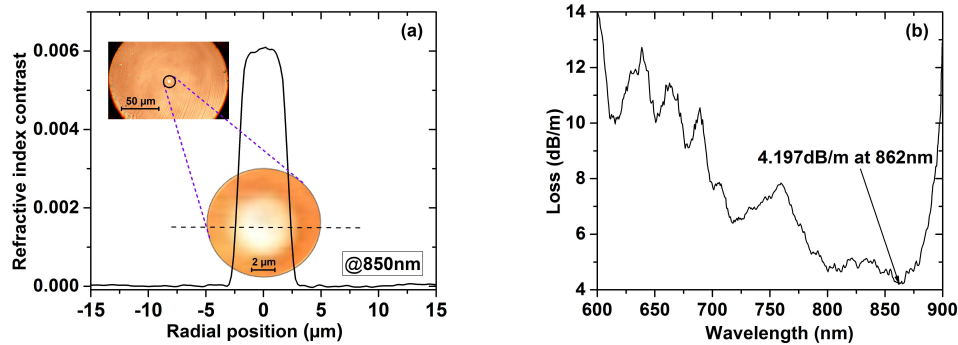


Fig. 1. (a) Measured refractive index contrast of SIPOF at 850 nm. Inset: microscope image of the end facet of the SIPOF. (b) Measured transmission loss of the SIPOF.

3.2 Fiber Bragg grating inscription and characterization

In order to explore the potential of this fiber for sensing, fiber Bragg gratings were inscribed in the fabricated SIPOF. The technique we used for inscribing the grating was the phase mask technique and the configuration setup used is the same as described in reference [36]. The phase mask used for inscribing the grating in the SIPOF has a 572.4 nm uniform period, making it suitable for writing FBGs in polymers fibers in the 850 nm region using a He-Cd 325 nm laser. The laser power used for inscription was only 6 mW and the writing time was 4 minutes as shown in Fig. 2(b). Despite the low power of 6 mW the writing time was shorter than the shortest writing time of 7 minutes reported for PMMA microstructured POF using 30 mW [36] and it is much shorter than the writing time of 338 minutes reported in TOPAS microstructured POF [28], all using a CW He-Cd laser. It is here worth mentioning that a writing time of 30 seconds was achieved using a pulsed excimer laser [37]. The typical reflection spectrum of a 2 mm long grating inscribed in the single mode SIPOF is shown in Fig. 2(a). The Bragg wavelength is located at 869.53 nm with a reflection strength of 30 dB and a full width half maximum (FWHM) of 0.29 nm. Before characterizing it for humidity, temperature and strain, the SIPOF was annealed for 24 hours at 110°C. Figure 2(a) shows the reflection spectrum of the FBG before and after annealing.

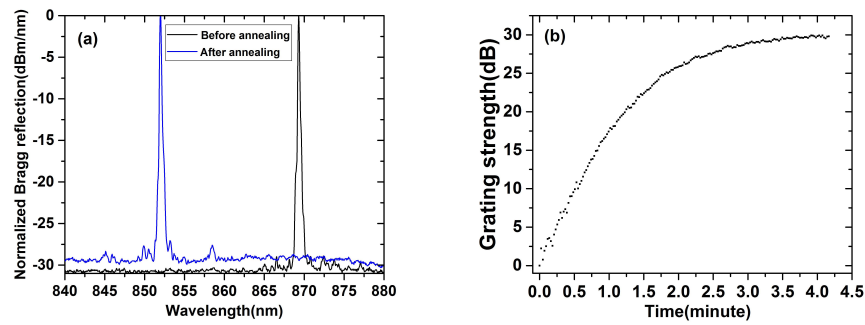


Fig. 2. (a) Bragg reflection of the SIPOFBG before and after annealing both normalized to the power of non-annealed grating. (b) Growth dynamic of the peak intensity of the 2 mm SIPOFBG during writing.

To study the humidity response, the fiber was first connectorized with a silica patch cable, which is single mode in the 850 nm region, and then placed in an environmental chamber (CLIMACELL, MMM group), which has a precision better than 0.3°C and 1% RH for relative humidity levels of 10-90%. Figure 3 illustrates the setup, in which a supercontinuum source (NKT Photonics A/S) has been used as a light source and a spectrometer (CCS175 - Compact Spectrometer, Thorlabs) has been used to continuously track the FBG peak during the humidity test. The humidity measurement has been done at 25°C. The relative humidity (RH) was first increased from 10% to 90% in steps of 10%. The chamber was programmed to increase the RH by 10% gradually within 30mins and then to keep the environmental conditions stable for another 30mins. Hence the total time allowed before increasing the relative humidity by 10% again was one hour. At the end of the ramp, the fiber was left inside the chamber for 24 hours at 90% RH to further investigate its humidity response. The total wavelength shift throughout the whole investigation was 40.85 pm, of which 35.13 pm was the change resulting from the increase from 10 to 90% and the 5.72 pm was the shift observed during the constant 90% RH period (occurred in the first 5 of the 24 hours). For the remaining 19hours no significant change in the Bragg wavelengths was measured. The humidity sensitivity when the RH was increased from 10 to 90% RH is 0.45 ± 0.22 pm/%RH, which is 78 times smaller than the sensitivity given by a step index PMMA POFBG [23].

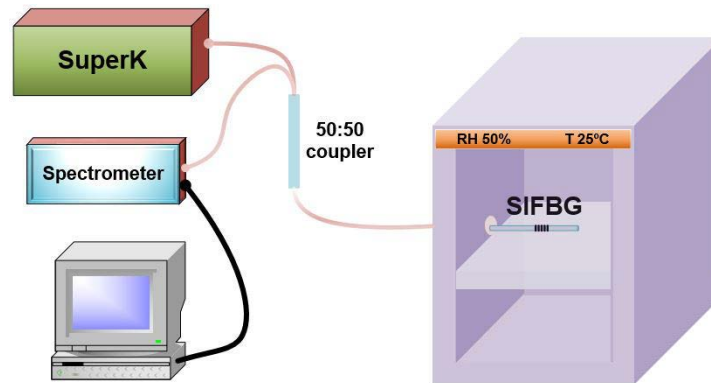


Fig. 3. Setup used for humidity and temperature measurement.

The temperature response of the SI POFBG was characterized with the same setup as the one used for humidity sensitivity measurements. The chamber was programmed to increase the temperature from 20°C to 105°C (the maximum operating temperature of the chamber)

and then to decrease down to 20°C, with a step of 5°C gradually within 5 minutes and stabilization time of 10 minutes at fixed 50% RH. Figure 4(b) shows the temperature response in the range 20°C to 105°C at 50% RH. The temperature sensitivity of this fiber is 17.57 ± 0.1 pm/°C for increasing temperature and 17.3 ± 0.02 pm/°C for decreasing temperature.

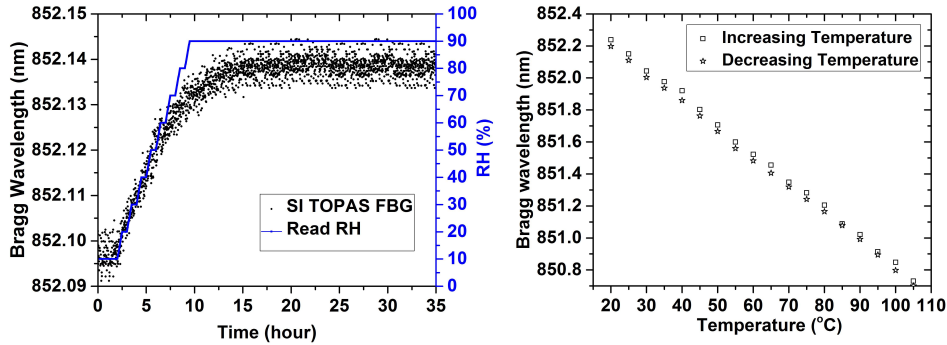


Fig. 4. (a) Humidity response of single-mode SIPOFBG at 25°C. (b) Temperature response single-mode SIPOFBG at 50% RH.

The strain response of the SI POFBG was studied by mechanically elongating the grating and monitoring its reflection spectrum. One end of the fiber was first connectorized with a single mode silica patch cable. Two centimeters away from the grating the fiber was clamped and glued to two micro-translation stages. One of the stages was used to apply axial strain manually to the grating. Every time strain was applied to the grating, 10 minutes were given for the grating to get stable before recording the reflection spectrum. The fiber was longitudinally strained up to 3% with steps of 0.25%. As shown in Fig. 5, the grating shows a linear response with an R-square value of 0.999 with no hysteresis. A linear fit of the results gives a strain sensitivity of 0.76 ± 0.02 pm/ $\mu\epsilon$, for both loading and unloading cases. This value matches the sensitivities of 0.71 pm/ $\mu\epsilon$ reported for PMMA 3-ring mPOF FBGs at 850 nm [18] and 827 nm [38].

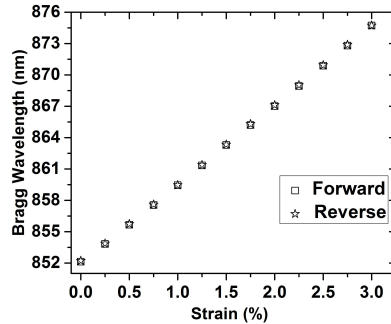


Fig. 5. Strain response of single-mode SIPOFBG.

4. Conclusion

In this work, we have fabricated for the first time a step-index single mode and humidity insensitive polymer optical fiber using injection molding technique. This technique provided a fast and flexible method of preparing step index preforms. The fabricated step index polymer optical fiber has a core made from TOPAS 5013S-04 with a glass transition temperature of 134°C and a cladding from ZEONEX 480R with a glass transition temperature of 138°C. The core and the cladding diameters of this fiber are 4.8 μm and 150 μm ,

respectively, which is compatible with a standard single mode silica fiber in the 850 nm region. The step index fiber has a minimum attenuation of 4.197 dB/m at 862 nm, which we anticipate can be further reduced by improving the preform production process. A fiber Bragg grating has also been inscribed in the proposed fiber in 4 minutes with as little as 6mW power from a CW He-Cd laser. We believe that FBGs inscribed in this step index fiber are particularly suitable for sensing applications that require high operating temperature and very low moisture absorption.

Acknowledgments

The research leading to these results has received funding from the People Programme (Marie Curie Actions) of the European Union's Seventh Framework Programme FP7/2007-2013/ under REA grant agreement n° 608382. The authors also acknowledge financial support from Innovation Fund Denmark for the project ShapeOCT (J. No. 4107-00011A), the Eugen Lommel Stipend for financial support and Danish Council for Independent Research (FTP Case No. 4184-00359B).